International Journal of Research Publication and Reviews Vol (2) Issue (7) (2021) Page 362-379

International Journal of Research Publication and Reviews

Journal homepage: www.ijrpr.com ISSN 2582-7421

Parametric Optimization in Wire Electrical Discharge Machining of EN-8 Material using Taguchi's Methods

Ambuj Shukla[a]*, *Sumit Dwivedi*[a]

[a]*Department of Mechanical Engineering, B. N. College of Engineering and Technology Lucknow (U.P) – 226201,India*

A B S T R A C T

WEDM (Wire Electrical Discharge Machining) is widely utilized in the machining of conductive materials where complicated and complicated geometries with better dimensional precision and surface polish are required. Aerospace, automotive, mold-making, and medical sectors are among the industries with applications. WEDM has remained a competitive and cost-effective machining method through the years, meeting the machining needs imposed by short product development cycles and rising cost demands. With the advancement of the mechanical sector, there is a growing demand for alloy materials with high hardness, toughness, and impact resistance. In the previous two decades, the machine tool industry has seen exponential expansion in its production capabilities, but machine tools are still underutilized. The failure to run the machine tools at their optimal operating conditions is the cause of this constraint. For a long time, the challenge of arriving at a precise analysis of the operational parameters has piqued the interest of researchers and working engineers. For WEDM of EN-8 steel, a single response optimization technique based on Taguchi's methodology is suggested in this work. Material removal rate (MRR) and surface roughness (SR), as well as the surface shape of the machined surface, are the machining variables being researched. The experimentation in this study was designed and carried out according to Taguchi's design approach (L9 Orthogonal array). The pulse-off-time, peak current and pulse-on-time, were all varied in the experiments. The MRR and SR in the wire electrical discharge machining of EN-8 steel were investigated using an orthogonal array, the signal-to-noise (S/N) ratio, and analysis of variance (ANOVA). MRR and SR, as well as surface morphology (SM), were shown to be important factors in the study. The following conclusion may be derived from this study: MRR reduces as pulse off time grows, and surface roughness rises initially, then lowers as pulse on time grows. In a microstructure investigation, Crater rises on a machined surface as the pulse on time grows, whereas Debris grows as the peak current increases and the pulse off time decreases. Crakes can also occur as a result of uneven heating or cooling.

Keywords: Wire Electrical Discharge Machining,EN-8 steel, Analysis of variance (ANOVA), Material removal rate (MRR),Surface roughness (SR)

1. Introduction

WEDM is a kind of EDM that makes use of an extremely thin wire as the electrode. Special brass wires are often used; the wire is carefully inserted into the material, and electrical discharges cut the work piece. WEDM is commonly done in a water bath. The wire does not actually touch the metal to be cut in the WEDM process under a microscope; Small quantities of material are removed by the electrical discharges, allowing the wire to pass through the workpiece. The intense heat in the zone causes the materials in the sparking zone to melt and evaporate. A discharge occurs between two sites of the anode and cathode(Ho et al., 2004).

WEDM is a well-known non-traditional material removal method for creating intricately profiled components. A sequence of electrical discharges is created between a properly positioned moving wire and the work piece in WEDM to manufacture conductive materials. Through an insulated dielectric fluid (DF) with a very small spark gap, DC or high frequency pulses of AC are discharged from the wire to the work piece. The WEDM method takes advantage of the complicated erosion effect of fast recurring and discrete spark discharges between the wire tool electrode and the work piece immersed in a liquid dielectric medium. WEDM is used to make aircraft parts such as small gas turbine blades and electronic components (Anand, 2016).

Wire electrical discharge machining is a particular thermal machining process capable of correctly cutting components with changing hardness or complicated forms, as well as pieces with sharp edges that are difficult to produce using traditional machining methods. WEDM is now a widely utilised process in industry for highprecision machining of all sorts of conductive materials of any hardness, including metals, metal alloys, ceramic materials and

* *Corresponding author.* Tel.: +91-7985603552;
E-mail address: yashushukla034@gmail.com

even some graphite. The Ip, which uses low power for ignition and high power for milling, has been used by several Wire-EDM machines. However, no matter how short the Ton is set, the energy released by the high-voltage subcircuit is too high to achieve a desirable well surface, making it unsuitable for finishing (Ho et al., 2004)(Anand, 2016).

This machining technology is typically used for extremely rigid metals that are difficult to mill using traditional procedures. It's been frequently employed, particularly for cutting intricate curves or tiny cavities that are difficult to achieve with traditional machining procedures. However, WEDM only works with electrically conductive materials, which is a significant constraint. A computer usually controls the wire's route, allowing for the creation of exceedingly intricate forms. The desired form is created using a wire electrode in the WEDM process. The wire is inserted into the component in the same way that a cheese cutter is inserted into cheese. Copper wire is nearly usually used, and because copper wears quickly, it is supplied on reels. Brass, copper, or tungsten wires are commonly used, as are brass or zinc-coated and multi-coated wires. The wire's movement is controlled by a computer on two axes (and sometimes more). This is the same as any other CNC controlled procedure, only the form is formed independently by directing the wire in CNC EDM (Anand, 2016)(Puri & Bhattacharyya, 2005)(Abinesh et al., 2014).

The most well-known and non-traditional machining technology in use today is wire electrical discharge machining. A series of discrete sparks (DS) between the work piece and the wire electrode erode the material off the work piece, separated by a thin film of DF that is continuously supplied to the machining zone to flush away the eroded particles in WEDM. The tool electrode and the work are retained at a precise distance from one another, called the spark gap, which varies according on the operating circumstances. This space prevents the tool from making mechanical contact with the work. The movement of the wire is mathematically controlled to accomplish the work piece's 3-dimensional form and precision. Figure 1 shows a schematic illustration of WEDM. Wire electrodes are often constructed of tungsten, copper or brass, and have a diameter of 0.050mm to 0.30mm, allowing for extremely tiny corner radii. The latter breaks down when the equipulsed voltage is supplied between the two electrodes separated by dielectric fluid. The released electrons are accelerated in the presence of an electric field and crash with dielectric molecules, robbing them of their electrons. With secondary emission, the process multiplies, resulting in an avalanche of electrons and ions. As the dielectric layer is ionised, its resistance decreases, leading in final breakdown. The electric energy is discharged into the gap, causing a cascade of events. Electro-dynamic waves begin to form and propagate at a high rate, creating shock and a rapid rise in temperature at the electrodes' surfaces. The temperature can exceed 10,000 0C in a second, producing localised vaporisation of the electrodes(Puri& Bhattacharyya, 2005).The literature on wire-cut electrical discharge machining is categorized into distinct models based on the authors' approaches and solution approach. Figure 5 is a pie chart depicting the percentage distribution of wire-cut electrical discharge machining literature analyzed. It is shown that empirical models are used in 26% of the research, whereas distinct optimization models are used in 21% of the research. Only 12% of the papers reviewed used artificial intelligence models to improve WEDM process performance. It was discovered that 22% of the literature examined uses a technical change to the fundamental wire-cut electrical discharge machining procedure. In terms of numerical and analytical models, the graph demonstrates that only 7% and 14% of work in the WEDM process, respectively. Only 2% of study effort in the wire electrical discharge machining taper cutting process has used logical models, 1% of research work has used mathematical models, and 1% of research work has used mathematical models, according to the literature for WEDM straight cutting and taper cutting. As a result of identifying the gap in the literature, the proposed study plan was born(Anand, 2016)(Garg, 2010)(Ramakrishnan & Karunamoorthy, 2006)(Puri & Bhattacharyya, 2003).

The influence of changing a process parameter on MRR, SR, and surface integrity is summarized in this research review. According to the literature, increasing the Ton and Ip improves MRR and SR, whereas increasing the Toff reduces MRR and SR. When the Ton is increased, the crater on the machining surface grows, a fracture forms on the machining surface owing to uneven heating or cooling, and debris forms owing to a rise in Ip and a reduction in Toff. The Ton, Toff and Ip are chosen for this study based on the aforementioned research parameters to examine the MRR, SR (surface roughness) and SM using the Taguchi design methodology(Abinesh et al., 2014)(Garg, 2010)(Rao et al., 2014)(Goswami & Kumar, 2014)(Vikas et al., 2014).

• Using Pulse-off-time, Pulse-on-time, and peak current to improve the MRR
• Using Pulse-off-time, Pulse-on-time, and peak current to improve SR
• Using Pulse-off-time, Pulse-on-time, and peak current to analyses SM

Nomenclature

WEDM	Wire cut Electrical-Discharge Machining
EDM	Electrical-Discharge Machining
CNC	Computer numerical control
MRR	Material removal rate
Ton	Pulse-on-time
Toff	Pulse-off-time
Ip	Peak current
ANOVA	Analysis of variance
SR	Surface roughness
µsec	microsecond
A	AMPERE
DF	Dielectric fluid
DS	Discrete sparks
IEG	Inter Electrode Gap

WF	Wire feed
SRM	Response Surface Methodology
ANFIM	Adaptive neuro-fuzzy inference method
CV	Cutting velocity
MR	Machining rate
OA	Orthogonal arrays

2. Experimental design

For effective experimentation, a scientific method to planning the tests is required. Statistical design of experiments is used to organise the experiment, ensuring that relevant data is collected and analyzed using numerical methods, resulting in trustworthy and objective results. When the problem involves data that has been subjected to experimental error, numerical analysis is the only objective method of analysis. An experimental challenge consists of two parts: the design of the experiments and the numerical analysis of the results. These two principles are intertwined since the technique of analysis is directly dependent on the experiment design. The following are some of the benefits of experiment design:

- The number of trials has been drastically decreased.
- Important decision factors that govern and improve the performance of the product
- It is possible to determine the best parameter settings.
- Parameters can be estimated qualitatively.
- It is possible to calculate the experimental error.
- It is possible to make inferences about the influence of factors on process characteristics.

The Taguchi technique was used to organize the trials and the subsequent analysis of the data acquired in this study.

3. Taguchi design of experiment

Minitab 14 was used to create the experiment design. Table 1 shows the experiment's design(Equbal et al., 2014).

Table 1- L9 Orthogonal Array

Exp. No	Ton	Toff	Ip
1	106 µsec	30 µsec	80 A
2	106 µsec	42 µsec	120 A
3	106 µsec	54 µsec	160 A
4	112 µsec	30 µsec	120 A
5	112 µsec	42 µsec	160 A
6	112 µsec	54 µsec	80 A
7	118 µsec	30 µsec	160 A
8	118 µsec	42 µsec	80 A
9	118 µsec	54 µsec	120 A

Table 2- Parameters and their levels

S.No.	Parameters	Level 1	Level 2	Level 3	Units
3	Peak Current	80A	120A	160A	A
1	Pulse-on-time	106 µsec	112 µsec	118 µsec	µsec
2	Pulse-off- time	30 µsec	42 µsec	54 µsec	µsec

4. EXPERIMENTAL DESIGN

On an ELPULS15 Electronica Ecocut Wire-EDM machine, experiments are carried out. Figure 1 depicts the machine. The wire electrical discharge machine belongs to the category of machining processes known as "non-traditional" or "non-conventional." Wire- cut EDM may be thought of as a series of liquid dielectric breakdowns and repairs in the space between the electrodes. The machine is accessible in Qaiserbagh Lucknow's "Maryam Engineering Works." Table 3 lists the machine's specifications.

Table 3 Specifications of ELPULS15Electronica Ecocut WEDM

Design	Fixed column, moving table
Best surface finish	1.2 μm R_a
Input power supply	3 phase,50 Hz , AC 415 V
Max. table size	370 x 600 mm
X & Y travel	250 x 350 mm
Controlled axes	X,Y,U,V simultaneous/Independent
Taper	5^0 over 100 mm
Max. work height	200 mm
Wire electrode diameter	0.20mm (optional),0.25 mm (standard), 0.15 mm
Max. cutting speed	370 mm/min
Generator	ELPULS-40 A DLX
Average power consumption	6-7 KVA
Interpolation	Circular and Linear
Connected load	10 KVA

Fig.1-Experimental setup of wire-cut electrical discharge machining

Fig.2- Nearer view of machining region

5. WORK PIECE MATERIAL

Table 4: Properties of EN-8 steel

Yield Strength	Density (g/cm^3)	Tensile Strength	Brinell Hardness	Impact Strength
465 N/mm^2	7.85	700-850N/mm^2	201-255	28J

Table 5: Chemical composition of EN-8 steel material (% by weight)

Material	Manganese	Carbon	Phosphorus	Silicon	Sulphur
Percentage	0.60-1	0.36-0.44	0.05Max	0.1-0.4	0.05Max

Tables 4. and 5. illustrate the properties of work-piece EN-8 steel and chemical composition respectively. It's found in automotive and aeronautical parts, as well as connecting rods, axels, spindles, bolts, and other technical elements. It has a good tensile strength, is easy to machine, and has a moderate wear resistance when heat treated. By using flame or induction hardening techniques, EN8 may be heat treated to give an excellent SR and moderate wear resistance.

6. TOOL MATERIAL

The experiment was carried out using a “Electronica Ecocut wire-cut electrical discharge machining” machine using brass wire with a diameter of 0.25 mm. The 6 mm flat work piece materials are installed on the Electronia Ecocut wire-cut electrical discharge machining machine tool, and a 10x10x6mm specimen is cut out with brass wire.

7. MEASUREMENTS

The goal of this paper is to improve the SR, SM and MRR, as shown below.

7.1. Material Removal Rate

The MRR is the rate at which material is removed from a workpiece. Some material is liquefied and then evaporated during machining, depending on the process settings of the EDM. By multiplying the weight loss of the work piece (in grammes) by the product of the work piece density and the machining time, the MRR can be calculated. The greater the pace of material removal, the better the productivity. As a result, increasing the MRR is highly desirable. The MRR formula is as follows.

MRR=(Work piece weight loss (gm) X 1000)/(Machining Time(min) x Density (gm/cc))

7.2. Surface Roughness (SR)

SR indicates how well a project was machined. It is desired to reduce the workpiece's surface roughness because when the surface roughness is reduced, the workpiece's surface finish improves and the machining quality improves. The TR200 surface roughness tester is used to quantify surface roughness. This is offered at Lucknow's "BBD University, Lucknow" The TR-200 SR tester is depicted in Figure 3, and the SR setup characteristics are shown in Table 6.

Fig.3-TR-200 surface roughness tester

Table 6 Specifications of surface roughness tester

Model No	TR-200
Accuracy	≤ ± 10%
Roughness parameters	Ra, R3z, Ry, Rp, Rq, Rz, Rt, Rv, RS
Display resolution	0.010 μ m
Measuring system	Imperial, Metric
Measuring Range	Ra: 0.025 μm ~12.50μm
Tracing length	(1~5) L + 2L
Digital filter	Gauss, D-P, RC, PC-RC,
Cutoff length (L)	0.25mm / 0.80mm / 2.50mm/Auto
Assessed profiles	Roughness profile (R)

The sensor travels linearly along the recorded length throughout the measurement operation. The probe moves in accordance with the surface profile. An A/D converter amplifies, filters, and converts these motions into electric impulses. These signals are then processed in the main processor and shown as Ra and Rz values on the screen.

7.3. Surface Morphology

The scanning electron microscope is a versatile analytical microscope with a large specimen chamber that can handle large specimens at the analytical working distance of 8.50mm, thanks to a combination of tilted detectors and a sharp conical objective lens(Shah et al., 2013). The SM was observed using the "CARL ZEISS EVO 50" SEM equipment. Figure 4 depicts this equipment. This is provided in the MSE department of "IIT Kanpur." The Description are given in table 7.

Table 7 CARL ZEISS EVO 50 SEM instrument specifications

X-ray Analysis	8.50 mm Analytical Working Distance (AWD) and 35° take-off angle
Magnification	5.00 x to 1,000,000x
Resolution	2.00nm@ 30.00Kv
Field of View	8.50 mm at the AWD
Acceleration Voltage	0.20 to 30 Kv
Detectors	SE in HV - Everhart-Thornley BSD in all modes - quadrant semiconductor diode

Fig.4-CARL ZEISS EVO 50 SEM instrument

SEM requires particular sample preparations, as stated below, because it employs vacuum conditions and an electron beam to generate an image.

• Because water will evaporate in the vacuum, all water must be eliminated from the samples.

• Non-conductive samples must be sputter coated with a tinny layer of conductive material such as Au /C/Ag to make them conductive.

• Electrically conductive samples do not require preparation before use, but they must be completely dry and free of volatile chemicals.

• The sample is taped to the surface of the stub with carbon tape. The sample is approximately 1 × 1 centimeter in size.

8. MACHINING PARAMETERS

Ip, Ton, and Toff are the key variables that affect the process mechanics in WEDM.

8.1. Peak Current

The Ip produced by the power supply is this. As the current rises, the amount of energy given rises as well. Higher energy raises the temperature of the work surface, resulting in a faster rate of material removal. The following are the Ip relationships:

• The material removal rate decreases as the peak current decreases. Due to insufficient work piece heating and short pulse length, the discharge energy produced between the working gap is minimal.

• At long pulse durations, material removal rate increases as the Ip increases.

• A rough surface is generated when the Ip and/or Ton are both high.

In my paper, the Ip varies between 80A, 120A, and 160A.

8.2. Pulse on time

It is the measurement of time in microseconds. Current is permitted to flow via the electrode towards the work material inside the spark gap during this time. The amount of energy delivered during the on-time period is directly related to the MRR. Longer pulse length enhances the rate of debris removal from the machined region, which has an impact on electrode wear behaviour. In my paper, I altered the pulse on time from 106µ seconds to 112µ seconds to 118µ seconds.

8.3. Pulse off time

The period in microseconds between the onset of two continuous sparks is referred to as Toff. During this stage of the cycle, there is no voltage. With a shorter pulse off time, more discharges may be made in a given amount of time, increasing sparking efficiency. As a result, the rate of cutting rises. However, using a very low Toff duration might result in breakage, which affects cutting efficiency. In my paper, I experimented with pulse off times of 30µ seconds, 42µ seconds, and 54µ seconds.

9. Result and discussion

9.1. Calculation for material removal rate

MRR is computed by multiplying the weight loss of the work piece (in grammes) by the product of the workpiece density and the machining duration. The values of MRR may be calculated using the relation, as given in table 8.

Table 8-Calculation of material removal rate

Exp. No	Toff	Ton	Ip	M/c Time	Work piece Wet loss	MRR
1	30(µsec)	106(µsec)	80(A)	16.18 minute	0.53 gm	4.19 mm³/min
2	42(µsec)	106(µsec)	120(A)	16.36 minute	0.53 gm	4.17 mm³/min
3	54(µsec)	106(µsec)	160(A)	19.30 minute	0.53 gm	3.52 mm³/min
4	30(µsec)	112(µsec)	120(A)	12.42 minute	0.53 gm	5.52 mm³/min
5	42(µsec)	112(µsec)	160(A)	14.53 minute	0.53 gm	4.72 mm³/min
6	54(µsec)	112(µsec)	80(A)	31.85 minute	0.53 gm	2.12 mm³/min
7	30(µsec)	118(µsec)	160(A)	10.98 minute	0.53 gm	6.14 mm³/min
8	42(µsec)	118(µsec)	80(A)	23.90 minute	0.53 gm	2.83 mm³/min
9	54(µsec)	118(µsec)	120(A)	25.17 minute	0.53 gm	2.69 mm³/min

9.2. Calculation of S/N ratio for material removal rate

The S/N ratio, which reduces the number of data points in a trial, is determined by the sort of attributes being assessed. The LARGERIS BETTER condition is used to analyze the S/N ratio for the material removal rate. Table 9. shows how to calculate the S/N ratio for MRR. The following equation is used to compute the S/N ratio for MRR:

$$S/NLB = -10\log\left((1/n)\Sigma\ (1/yi^{2})\right)$$

Table 9- Calculation of S/N ratio for material removal rate

S. No.	MRR	Signal to noise ratio
1	4.19 mm³/min	12.4443db
2	4.17 mm³/min	12.4027db
3	3.52 mm³/min	10.9309db
4	5.52 mm³/min	14.8388db
5	4.72 mm³/min	13.4788db
6	2.12 mm³/min	6.5267db
7	6.14 mm³/min	15.7634db
8	2.83 mm³/min	9.0357db
9	2.69 mm³/min	8.5950db

9.3. Calculation of Mean S/N ratio for material removal rate

$$\text{Mean S/N ratio } nfi = (nf1+nf2+nf3)/3$$

Where nf denotes the mean S/N ratio for factor f at level I of the given factor. The S/N ratios for factor f at level u are nf1, nf2, and nf3. The elements that influence machining parameters are shown in table 10 in order of importance. The value of delta determines the rank of the parameters. If one parameter's delta value is greater than the other, that parameter is ranked first. The ideal level of each element is indicated by a higher S/N ratio. In the above response table, Ip is the key influence, whereas pulse on time is less effective than Ip.

Table 10- Calculation of mean S/N ratio for material removal rate

Level	Ton	Toff	Ip
1	11.926(μsec)	14.349(μsec)	9.336 (A)
2	11.615(μsec)	11.639(μsec)	11.946(A)
3	11.131(μsec)	8.684(μsec)	13.391(A)
Delta	0.795	5.665	4.055
Rank	3	1	2

9.4. Analysis of Variance for material removal rate

Table 11-ANOVA of material removal rate

Source	DOF	Adj MS	Seq SS	F Value	% Contribution
Peak Current (μsec)	2	2.3308	4.6617	39.010	32.540
Pulse on Time (μsec)	2	0.0427	0.0854	0.710	0.5962
Pulse off Time(A)	2	4.7277	9.4555	79.130	66.020
Error	2	0.0597	0.11950		0.830
Total	8		14.3221		100.00

% of contribution= (SS /Total) X100

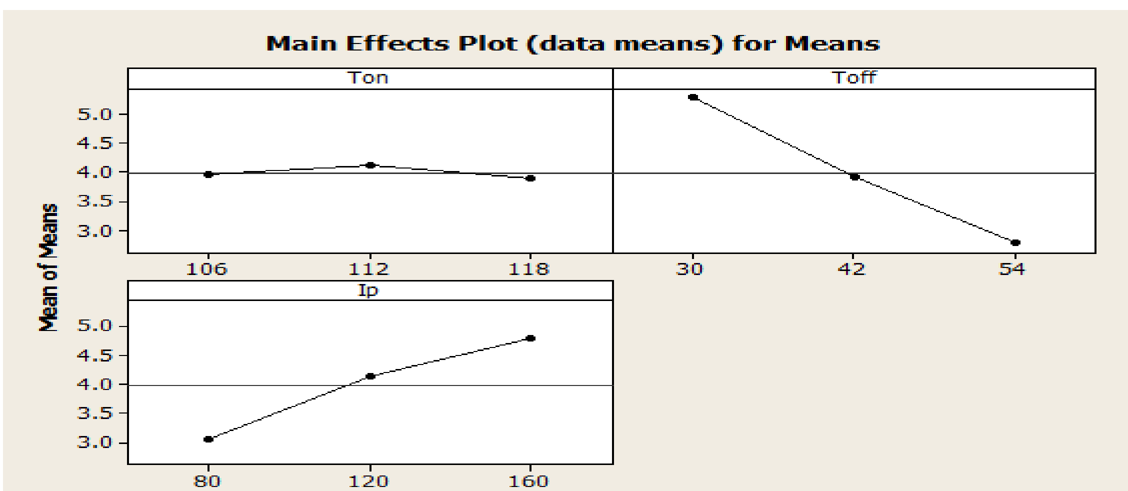

Fig.5-Main Effect Plot for material removal rate

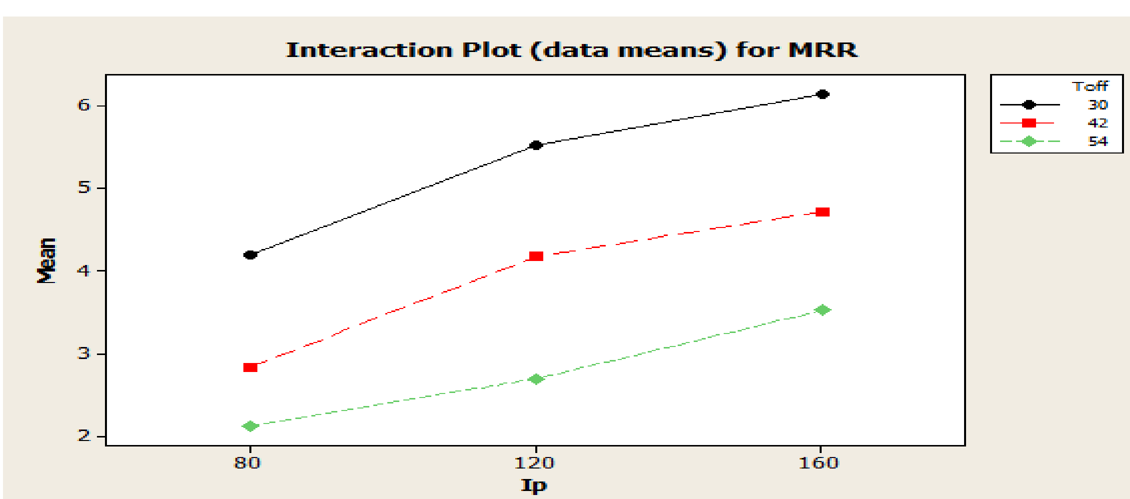

Fig.6-Interaction Plot for material removal rate

The material removal rate tends to grow at a high rate as the peak current is increased, as seen in figures 5 and 6. As a result, the rate of material removal rises.

9.5. Optimal level of parameter for material removal rate

The optimal level of parameters for material removal rate (MRR) is shown in table 12.

Table 12- Optimal level of parameter for material removal rate

Process variables	Optimum level
Ton	112
Toff	30
Ip	160

9.6. Calculation for surface roughness

Table 13 shows the calculation of SR varying with Ton, Toff and Ip.

Table 13-Calculation for SR

Exp. No	Toff	Ton	Ip	SR
1	30 µsec	106 µsec	80A	5.162 µm
2	42 µsec	106 µsec	120A	5.447 µm
3	54 µsec	106 µsec	160A	5.793 µm
4	30 µsec	112 µsec	120A	5.972 µm
5	42 µsec	112 µsec	160A	6.318µm
6	54 µsec	112 µsec	80A	6.712 µm
7	30 µsec	118 µsec	160A	5.652 µm
8	42 µsec	118 µsec	80A	4.254 µm
9	54 µsec	118 µsec	120A	5.388 µm

9.6.1 S/N ratio for SR

The S/N ratio, which reduces the number of data points in a trial, is determined by the sort of attributes being assessed. The SMALLER IS BETTER condition is used to analyze the S/N ratio for SR. The better the surface qualities, the lower the SR. Table 14. shows how to analyze the S/N ratio for SR. The S/N ratio for SR is calculated using the following equation:

$S/N_{SB} = -10\log\left(\left(1/n\right) \Sigma\, y_i^{2}\right)$

Table 14- S/N ratio for SR

S.No	SR	Signal to noise ratio
1	5.162 µm	-14.2547 db
2	5.447 µm	-14.7216 db
3	5.793 µm	-15.2566 db
4	5.972 µm	-15.5209 db
5	6.318µm	-16.0130 db
6	6.712 µm	-16.5357 db
7	5.652 µm	-15.0425 db
8	4.254 µm	-12.5739 db
9	5.388 µm	-14.6269 db

9.6.2 Calculation of Mean S/N ratio for SR

$$\text{Mean S/N ratio } \; n_{fi} = (n_{f1} + n_{f2} + n_{f3}) / 3$$

Where nf is the mean S/N ratio for factor f at the specified factor's level value i. The S/N ratios for factor f at level u are nf1, nf2, and nf3. Table 15. shows how to analyze the mean S/N ratio for SR.

Table 15- S/N ratio for SR

Level	Ton	Toff	Ip
1	-14.740 µsec	-14.940 µsec	-14.450A
2	-16.020 µsec	-14.440 µsec	-14.960A
3	-14.080 µsec	-15.470 µsec	-15.440A
Delta	1.940	1.040	0.980
Rank	1	2	3

9.6.3 Analysis of Variance for SR

Table 16: ANOVA of SR

Source	DOF	Seq SS	Adj MS	F Value	% Contribution
Pulse off Time(µsec)	2	0.5906	0.2953	1.10	14.780
Pulse on Time(µsec)	2	2.4180	1.2090	4.51	60.520
Peak Current(A)	2	0.4510	0.2255	0.84	11.280
Error	2	0.5357	0.2678		13.400
Total	8	3.9952			100

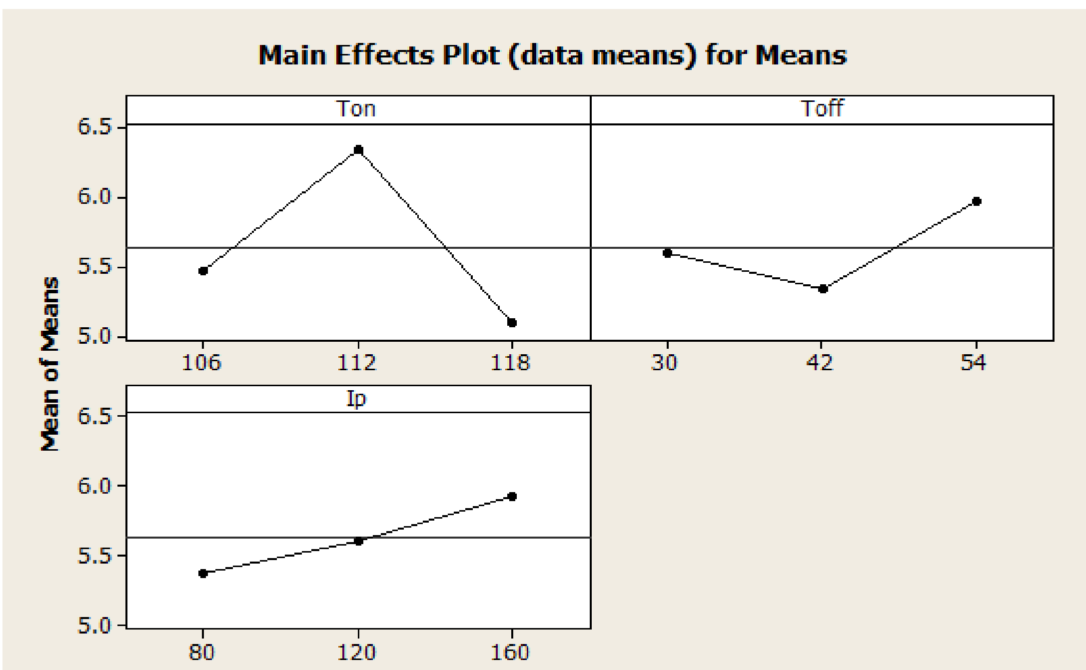

Figure 7. Main Effect are Plotted for SR

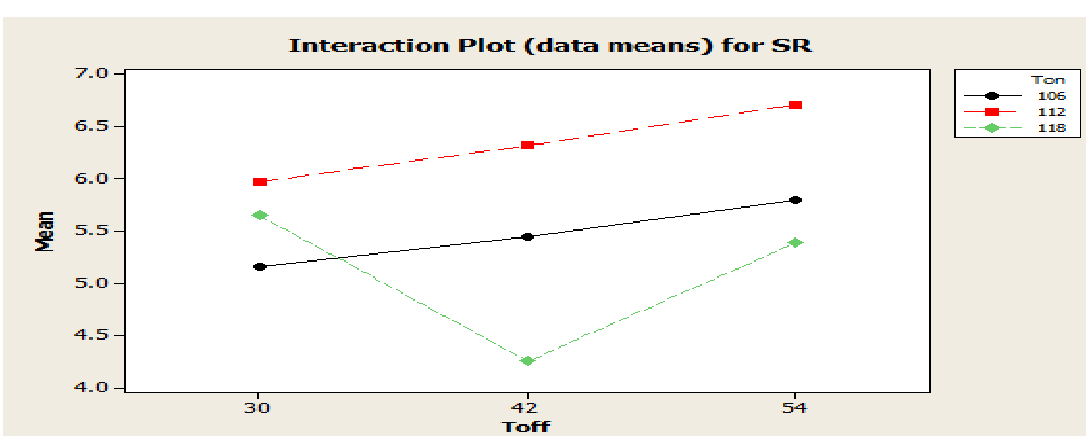

Figure 8Effects of Process Parameters Interactions on SR

The influence of input factors on surface roughness is shown in Figure 8. SR rises as peak current rises, and the surface smoothness begins to deteriorate. Because of the larger MRR, a very rough surface is formed as peak current is increased, resulting in a poor surface finish.

9.7. Selection of levels of parameter for surface roughness

For SR the optimum level of parameters is given in table 17.

Table 17- Optimal level of parameter for SR

Process variables	Optimum level
Ton	118 µsec
Toff	42 µsec
Ip	80A

9.8. *Confirmation of expected and actual values test*

Tables 18 and 19 show the results of confirmation tests for MRR and SR, as well as the optimal values of process variables.

Table 18- Confirmation of expected and actual values of material removal rate

Experiment No.	Optimum Machining Parameters			Material Removal Rate	
	Ton	Toff	Ip	Actual	Expected
1	112(µsec)	30(µsec)	160(A)	5.72 (mm^3/min)	5.66(mm^3/min)
				Error (%)	1.06%

Table 19- Confirmation of expected and actual values of SR

Experiment No.	Optimum Machining Parameters			Surface Roughness	
	Ton	Toff	Ip	Actual	Expected
2	118(µsec)	42(µsec)	80(A)	4.253	4.382
				Error %	3.03%

9.9. SURFACE MORPHOLOGY

9.9.1Microstructure of machined surface

The microstructure of a machined work surface was investigated in order to determine the surface quality obtained utilizing the WEDM method. A scanning electron microscope with an accelerating voltage of 10.00KV was used to examine the specimen. For microstructure analysis, all nine samples were chosen. Figures 9 and 10 depict the specimen and workpiece following WEDM.

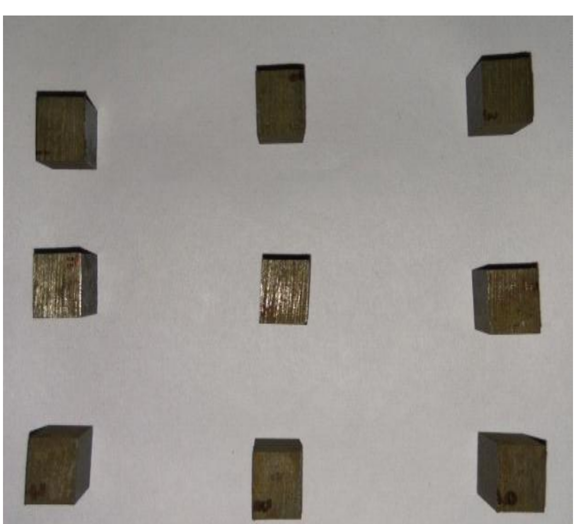

Fig. 9- Specimen of size 10x10x6 mm after wire electrical discharge machining

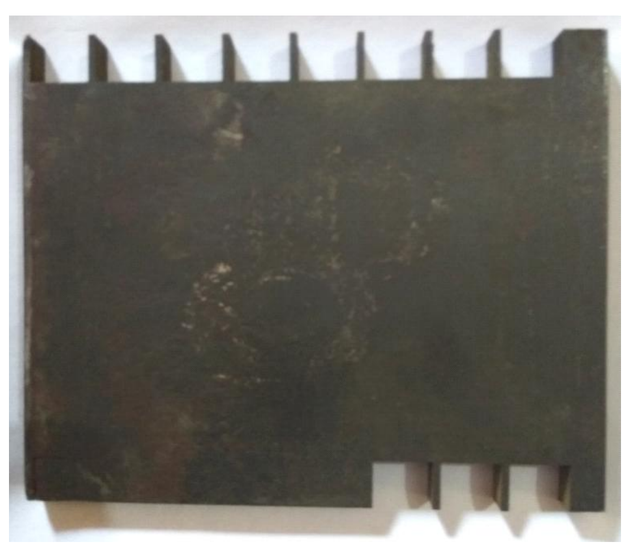

Fig. 10- Work piece after machining

First Sample

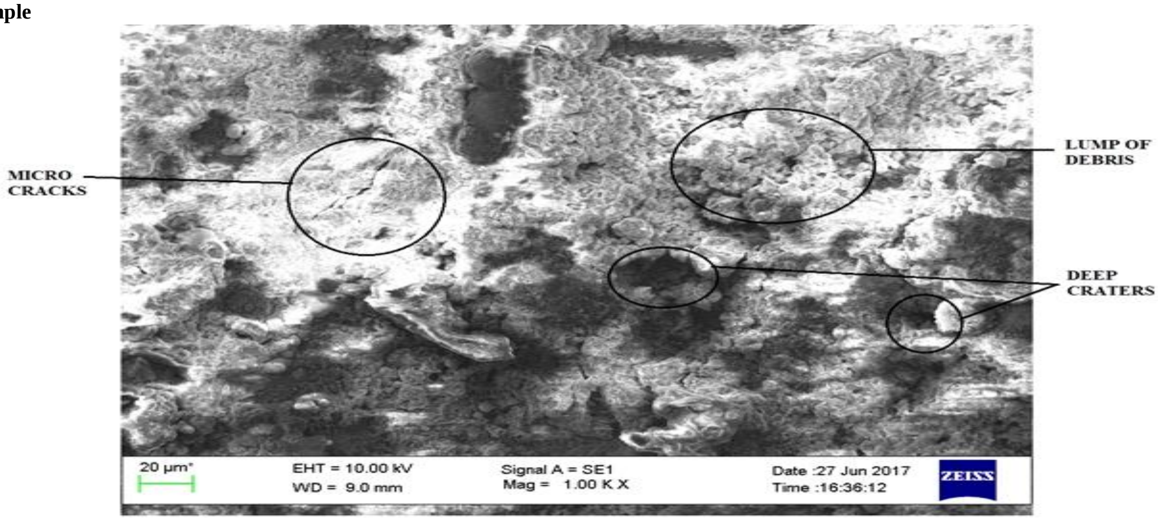

Fig. 11- Microstructure of the first sample

Figure 11 shows the microstructure of the first sample, which was machined under experimental conditions corresponding to a pulse-on duration of 106µ seconds, a Toff of 30µ seconds, and a peak current of 80 A. Because of the minimal heat input, the Ton, Toff, and Ip are all at their lowest levels.With a smaller current discharge, just a limited quantity of metal may be removed. The rapid heating and cooling of the machined surface is mostly to blame for the fracture development. Uneven heating and cooling led tensions to develop, resulting in fracture formation, lumps of debris emerge owing to inadequate flush pressure, and some deep craters occur on the machined surface of the work piece owing to vaporisation of metal.

Second Sample

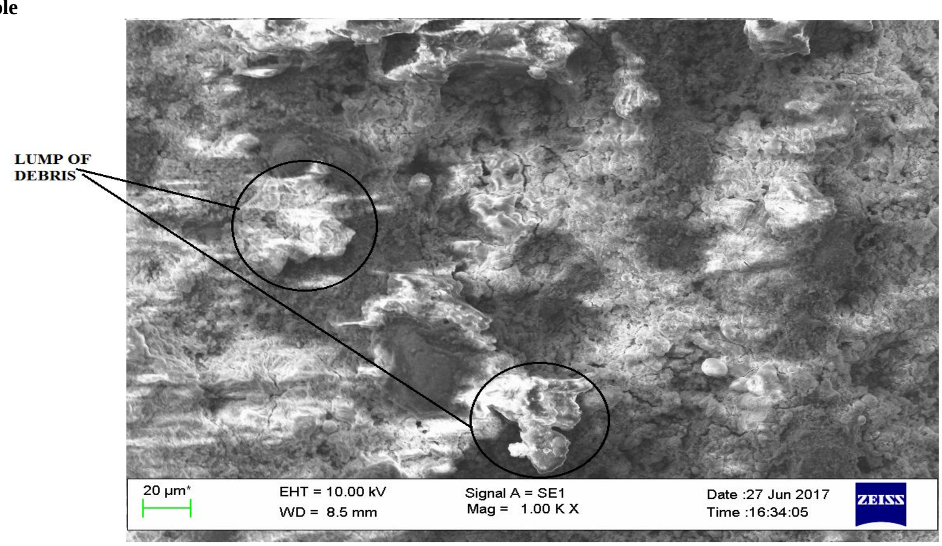

Fig. 12-Microstructure of the second sample

Figure 12 shows the microstructure of the second sample, which was machined under experimental conditions corresponding to a pulse-on duration of 106µ seconds, a pulse-off time of 42µ seconds, and a peak current of 120 A. The pulse-on-time was set to the lowest level, the Ton was set to a moderate level, and the Ip was set to a moderate level in this experiment. Because of the modest Ip, a tiny fraction of the material is heated to melting temperatures and redeposits on the surface due to incorrect flushing. The microstructure of this experiment shows a lot of lumps of detritus.

Third Sample

Figure 13 shows the microstructure of the third sample, which was machined under experimental conditions of 106µ seconds pulse on time, 54µ seconds Toff, and 160 A peak current. In this experiment, the Ton was set to the lowest level, the Toff was set to the highest level, and the peak current was set to the maximum level. Owing to the maximum degree of Ip, the impact of discharge energy on the work piece's surface is larger, resulting in increased surface degradation and a considerable amount of material flushed away due to the increased pulse off time. On the surface of the work piece, there is less probability of resolidification. As a result, a huge chunk of debris can be seen in the microstructure of this sample.

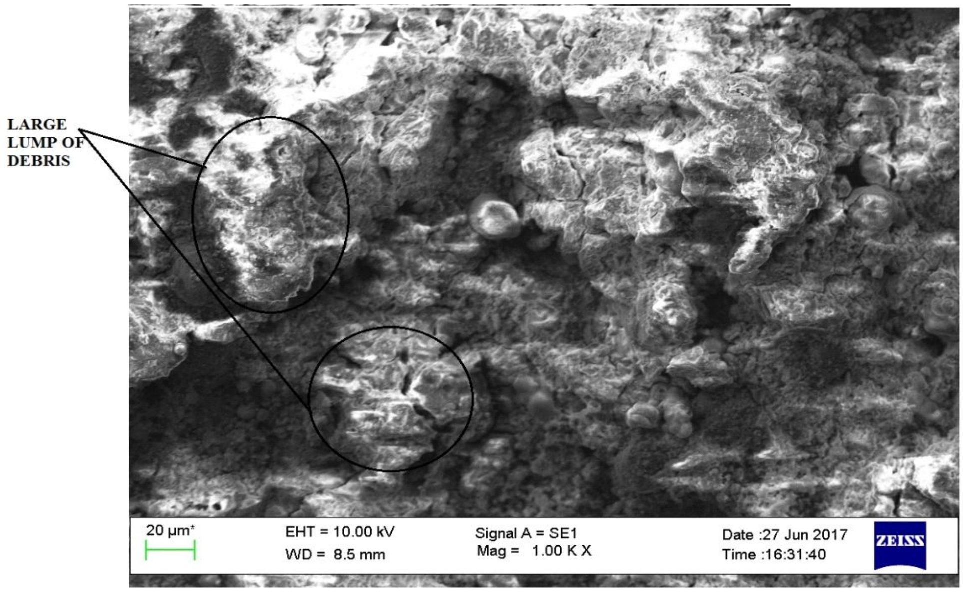

Fig. 13- Microstructure of the third sample

Fourth Sample

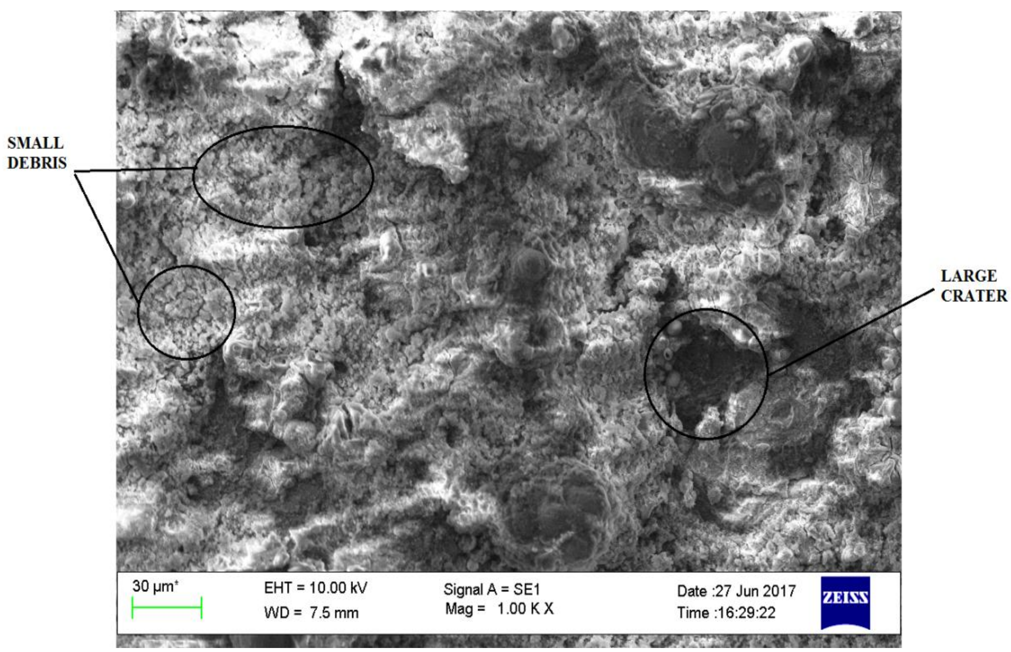

Fig. 14- Microstructure of the fourth sample

Figure 14 shows the microstructure of the fourth sample, which was machined under experimental conditions corresponding to a Ton of 112 seconds, a Toff of 30 seconds, and a Ip of 120 A. In this experiment, the Ton was kept at a moderate level, the Toff was kept at a low level, and the Ip was kept at a moderate level. Enhanced Ton results in a greater, more forceful explosion, resulting in increased MRR and quicker depletion; nevertheless, a minor increase in Ip erodes the work piece's surface. As a result, a large crater emerges on the machined surface of the work piece. There is a possibility of redeposit on the surface due to the short Toff, resulting in minute debris.

Fifth Sample

Figure 15. shows the microstructure of the fifth sample, which was machined under experimental conditions corresponding to a Ton of 112µ seconds, a Toff of 42µ seconds, and a peak current of 160 A. The Ton was kept at a moderate level, the Toff was kept at a moderate level, and the Ip was kept at the maximum level in this experiment. Erosion of the work piece occurs as a result of the modest Ton and greatest peak current, resulting in deep craters. Due to incorrect DF cleansing and uneven heating, small particles and micro fractures form. As a result, there's a potential that material will be redeposited, resulting in little debris on the machined surface.

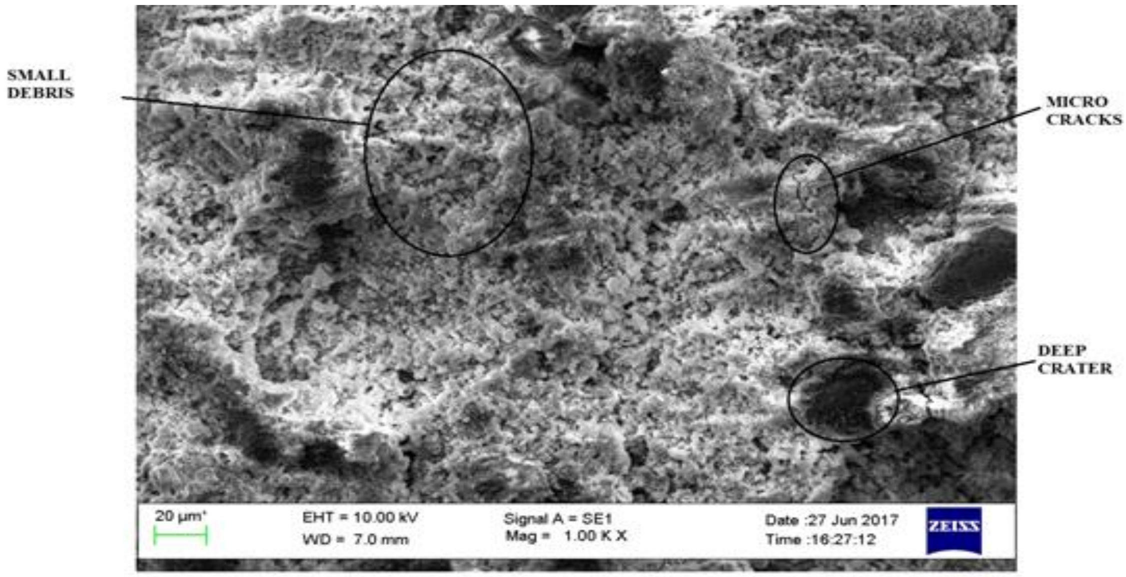

Fig.15- Microstructure of the fifth sample

Sixth Sample

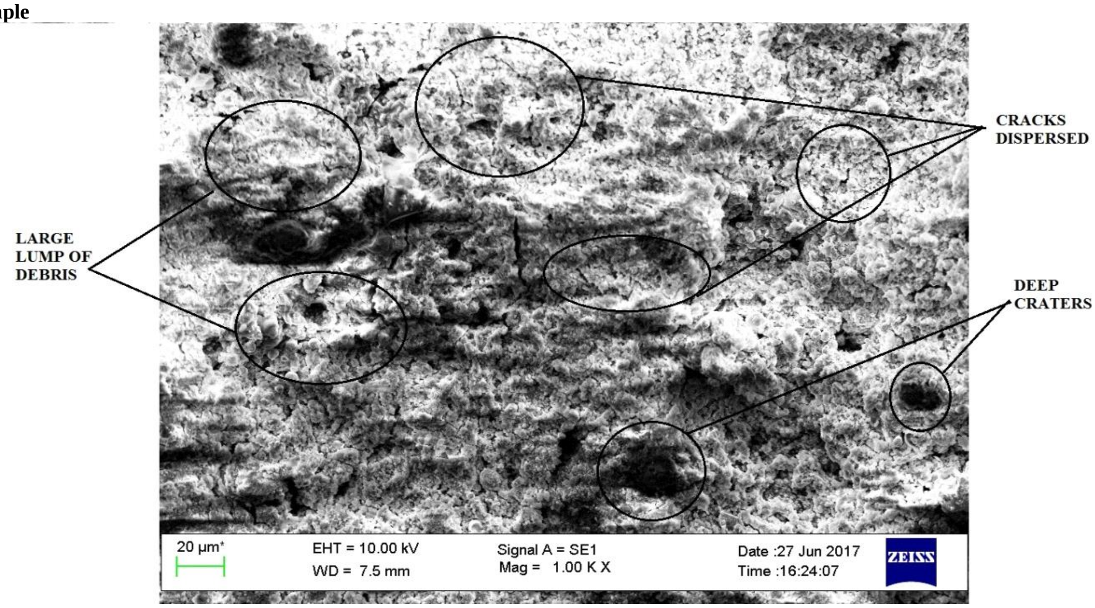

Fig.16- Microstructure of the sixth sample

Figure 16 shows the microstructure of the sixth sample, which was machined under experimental conditions corresponding to a Ton of 112µ seconds, a Toff of 54µ seconds, and a Ip of 80 A. The Ton was set to a moderate level, the Toff was set to the highest level, and the Ip was set to the lowest level in this experiment. The frequency of discharges rises due to intermediate Ton, which signifies a protracted period of Ip, resulting in deep craters. Due to incorrect DF flushing, large lumps of debris form, resulting in material resolidification. Large amounts of uneven cooling disseminate the fissures.

Seventh Sample

Figure 17 shows the microstructure of the seventh sample, which was machined under experimental conditions corresponding to a Ton of 118µ seconds, a Toff of 30µ seconds, and a peak current of 160 A. In this experiment, the Ton was set to the highest level, the Toff was set to the lowest level, and the Ip was set to the highest level. The most important characteristics impacting the surface attributes are Ton and Ip. The creation of craters on the surface was caused by an increase in Ton and Ip. These craters formed as a result of a prolonged period of spark duration, which increased the frequency of discharges, resulting in broader and deeper craters. The appearance frequency of these fractures is directly proportional to the machining circumstances; the higher the discharge energy, the more frequent these cracks emerge. Because cracking at high temperatures is caused by the phenomenon of segregation to solidification, which is caused by the enrichment in particular elements as solidification develops and internal stresses increase, these forms of cracking are caused by very high temperatures.

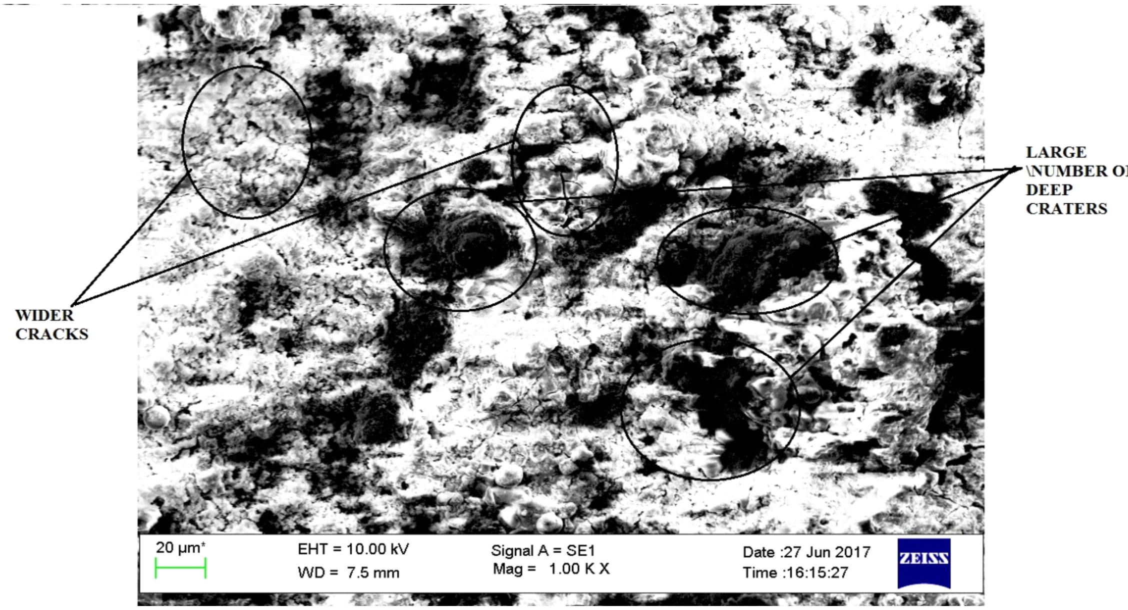

Fig.17- Microstructure of theseventh sample

Eight Sample

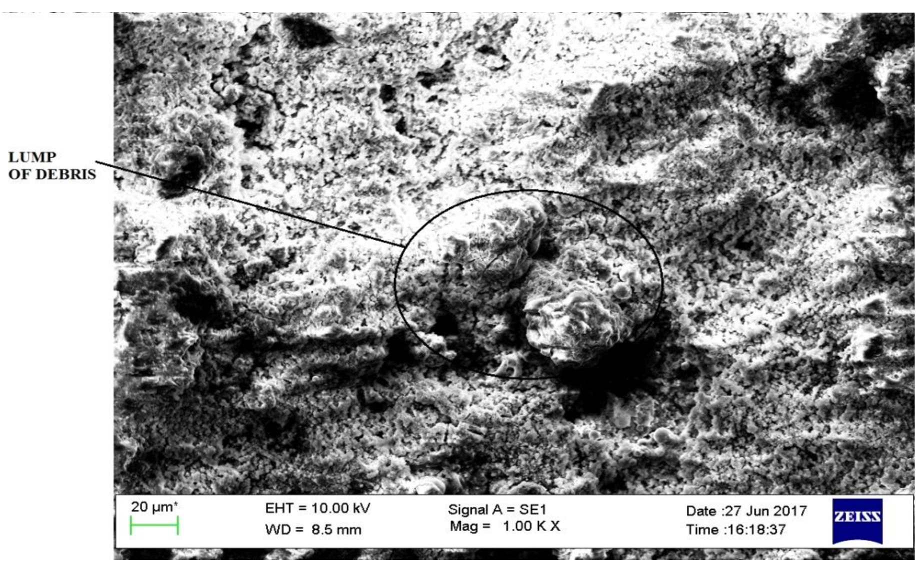

Fig.18- Microstructure of the eight sample

Figure 18 shows the microstructure of eight samples machined under experimental conditions of 118µ seconds Ton, 42µ seconds Toff, and 80 A peak current. Ton was set to the highest level, Toff was set to the intermediate level, and Ip was set to the lowest level in this experiment. With a prolonged period of spark duration and inadequate DF pressure in the flushing operation, a lump of debris appears on the machined surfa ce. There's a potential that some of the material will resolidify, resulting in clumps of debris on the studied surface.

Nineth Sample

Figure 19 shows the microstructure of the ninth sample, which was machined under experimental conditions corresponding to a Ton of 118µ seconds, a Toff of 54µ seconds, and a peak current of 120 A. The Ton was set to the highest level, the Toff was set to the highest level, and the Ip was set to the intermediate level in this experiment. Due to the maximum Ton and intermediate Ip, we see deep craters and debris on the machined surface. The creation of craters on the surface came from the rise in Ton and Ip. A series of sparks resulted in the formation of these craters. The DF eliminated a small percentage of the melted material created by the electric discharge. If the DF flushing pressure is inadequate. Then, on the studied surface, debris forms.

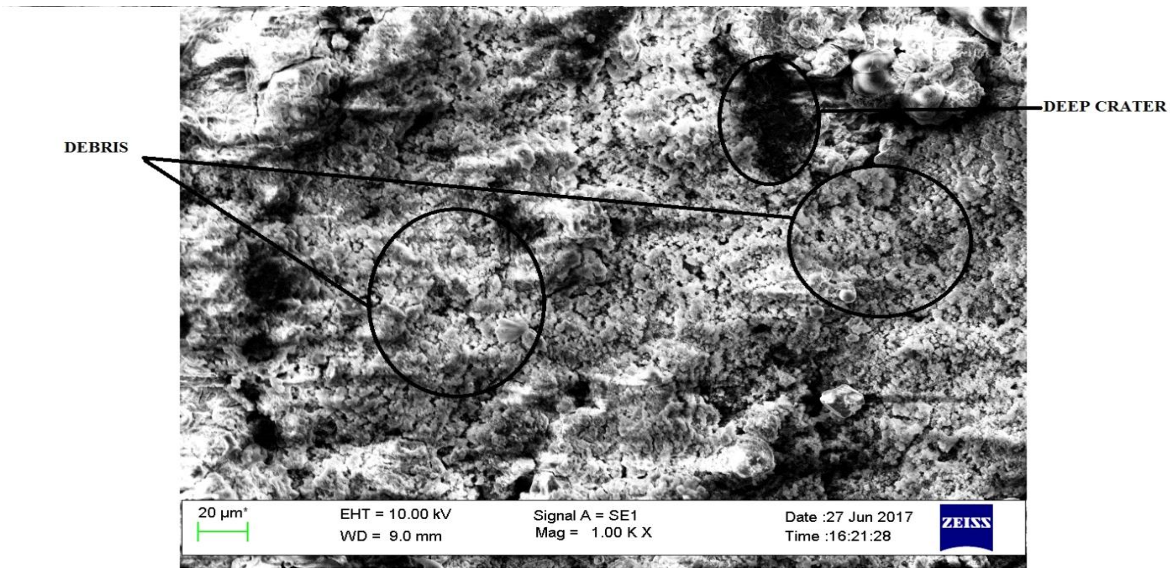

Fig.19- Microstructure of theninth sample

10. CONCLUSION

The purpose of this study is to see how cutting parameters affect the MRR and SR in the WEDM process. EN 8 is fairly machinable using the WEDM process, according to the results of this study. For two responses—material removal rate and surface roughness—optimized process conditions have been found. From this research, the following conclusions can be drawn. Surface roughness increases at first, then decreases with Ton, and material removal rate decreases as Toff increases. The impact of Toff on MRR is greatest and has a contribution of 66.02 percent. Second most predominant characteristic is Ip with a contribution of 32.54 percent. With a contribution of 0.5962 percent, Ton is the least influencing parameter on SR. With a contribution of 60.52 percent, Ton is the most influencing parameter on SR. Toff is the second most important factor, accounting for 14.78 percent of the total. Ip has the least impact, accounting for 11.28 percent of the total. In the SM study, craters increase with increased Ton due to increased discharge duration, while debris increases with increased Ip and decreased Toff. More material melted and evaporated as the Ip increased, increasing the value of current and hence the spark energy. Increased Toff reduces surface roughness since no spark is created during this period and material is flushed away, resulting in a smoother surface. Microcracks can also be seen as a result of uneven heating or cooling.

REFERENCES

Abinesh, P., Varatharajan, K., & Kumar, G. S. (2014). Optimization of Process Parameters Influencing MRR , Surface Roughness and Electrode Wear During Machining of Titanium Alloys by WEDM. *International Journal of Engineering Research and General Sience*, *2*(4), 719–729.

Anand, S. (2016). *M . Tech . Thesis OPTIMIZATION OF QUALITY CHARACTERISTIC IN WIRE ELECTRICAL DISCHARGE MACHINING OF INCOLOY 800 USING TAGUCHI METHODS*. 214–216.

Equbal, M. I., kumar, R., Shamim, M., & Ohdar, R. K. (2014). A Grey-based Taguchi Method to Optimize Hot Forging Process. *Procedia Materials Science*, *6*(Icmpc), 1495–1504. https://doi.org/10.1016/j.mspro.2014.07.129

Garg, R. (2010). Effect of process parameters on performance measures of wire electrical discharge machining. *Mechanical Engineering Department*, *Ph.D.*, 284. http://nitkkr.ac.in/nit_kuk/docs/Ph.D._Thesis_by_Rohit_Garg.pdf

Goswami, A., & Kumar, J. (2014). Investigation of surface integrity, material removal rate and wire wear ratio for WEDM of Nimonic 80A alloy using GRA and Taguchi method. *Engineering Science and Technology, an International Journal*, *17*(4), 173–184. https://doi.org/10.1016/j.jestch.2014.05.002

Ho, K. H., Newman, S. T., Rahimifard, S., & Allen, R. D. (2004). State of the art in wire electrical discharge machining (WEDM). *International Journal of Machine Tools and Manufacture*, *44*(12–13), 1247–1259. https://doi.org/10.1016/j.ijmachtools.2004.04.017

Puri, A. B., & Bhattacharyya, B. (2003). *An analysis and optimisation of the geometrical inaccuracy due to wire lag phenomenon in WEDM*. *43*, 151–159.

Puri, A. B., & Bhattacharyya, B. (2005). Modeling and analysis of white layer depth in a wire-cut EDM process through response surface methodology. *International Journal of Advanced Manufacturing Technology*, *25*(3–4), 301–307. https://doi.org/10.1007/s00170-003-2045-8

Ramakrishnan, R., & Karunamoorthy, L. (2006). Multi response optimization of wire EDM operations using robust design of experiments. *International Journal of Advanced Manufacturing Technology*, *29*(1–2), 105–112. https://doi.org/10.1007/s00170-004-2496-6

Rao, P. S., Ramji, K., & Satyanarayana, B. (2014). Experimental Investigation and Optimization of Wire EDM Parameters for Surface Roughness, MRR and White Layer in Machining of Aluminium Alloy. *Procedia Materials Science*, *5*, 2197–2206. https://doi.org/10.1016/j.mspro.2014.07.426

Shah, C. D., Mevada, J. R., & Khatri, B. C. (2013). *Optimization of Process Parameter of Wire Electrical Discharge Machine by Response Surface*

Methodology on Inconel-600. *3*(4), 1–8.

Vikas, Shashikant, Roy, A. K., & Kumar, K. (2014). Effect and Optimization of Machine Process Parameters on MRR for EN19 & EN41 Materials Using Taguchi. *Procedia Technology*, *14*, 204–210. https://doi.org/10.1016/j.protcy.2014.08.027